

RESEARCH ARTICLE

Food grade silica nanoparticles cause non-competitive type inhibition of human salivary α -amylase because of surface interaction

Wut Hmone Phue  | Divya Srinivasan | Aneela Hameed | Varoujan Yaylayan | Saji George

Department of Food Science & Agricultural Chemistry, McGill University, Sainte-Anne-de-Bellevue, Quebec, Canada

Correspondence

Saji George, Department of Food Science & Agricultural Chemistry, McGill University, 21111 Lakeshore Road, Sainte-Anne-de-Bellevue, QC, Canada H9X3V9
Email: saji.george@mcgill.ca

Wut Hmone Phue and Divya Srinivasan contributed equally to this work.

Funding information

NSERC, Grant/Award Numbers: RGPIN-2017-04727, CRC/George/X-coded/248475

Abstract

Given the potential of ingested particles to interact with enzymes in oral cavity, we compared different grades of SiO₂ particles (food-grade and non-food grade nanoparticles (FG-SiO₂-NP, NFG-SiO₂-NP), and food grade microparticles (FG-SiO₂-MP)) for their interaction with human salivary α -amylase (HSA). There were differences in the agglomeration behavior and relative abundance of silanol and siloxane groups among different grades of SiO₂ particles where FG-SiO₂-NPs contained less cyclic siloxane groups but more silanol groups. Secondary structure and function of HSA were negatively impacted by FG-SiO₂-NPs. In order to verify if this inhibition is mediated through surface interactions, pristine particles were compared with those interacted with pure protein (bovine serum albumin-BSA) and with food matrix (milk) for HSA inhibition. BSA coating of SiO₂ particles ameliorated HSA inhibition, but milk interacted ones showed an enhanced the HSA inhibition because of the presence of milk protease suggesting the relevance of surface interactions in manifesting potential negative impacts of silica particles used in food.

KEYWORDS

enzyme inhibition, food grade SiO₂ particles, food matrix, human salivary α -amylase, nanoparticle-protein interactions, SiO₂ nanoparticle

1 | INTRODUCTION

Applications of nano-sized particles in food, pharmaceuticals and nutraceutical industries for enhancing the stability, quality, and the bioavailability of active ingredients and overall functions of the final product are increasing exponentially.^[1] The growing trend in the application of

manufactured nanoparticles in food and consumer products undeniably leads to human exposure through oral route. While the consequences of nanoparticles entering human body through oral route remains largely elusive,^[2] there are ample reasons for concern as emerging studies point towards potential negative health effect of nanoparticles applied in food.^[3,4] For instance, oral administration

This is an open access article under the terms of the [Creative Commons Attribution](https://creativecommons.org/licenses/by/4.0/) License, which permits use, distribution and reproduction in any medium, provided the original work is properly cited.

© 2020 The Authors. *Nano Select* published by Wiley-VCH GmbH

of titanium dioxide (TiO_2) nanoparticles was observed to induce preneoplastic lesions and promote aberrant crypt development in the rat colon.^[5] Similarly, nanoparticles of amorphous silica (SiO_2) had shown the potential to activate inflammasome^[6] and enhance intestinal permeability.^[7] Thus, while these studies indicate the potential health risks of nanoparticles, studies addressing the interaction of dietary nanoparticles with proteins of relevance to gastrointestinal system are grossly lacking.^[1,8]

Upon entry into the human body, particles encounter various biological fluids and ultimately their surface gets coated with a wide range of biomolecules—generally referred to as “corona.” Surface corona plays an important role in the biological identity of particles and influences their fate and transports them in the body.^[9,10] Proteins form a major portion of the biocorona formed on the particle surface. The presence of protein corona can affect the agglomeration behavior and surface chemistry of pristine particles with potential implications on biocompatibility of the particles.^[11] While ingested nanoparticles are likely to interact with salivary proteins, there are prominent knowledge gaps on its implications to the structure and function of salivary enzymes.

Human salivary α -amylase (HSA), the most abundant enzyme in human saliva is characterized by single polypeptide chain of ~475 amino acid residues, two sulfhydryl groups and four di-sulfide bridges. HSA initiates the digestion of complex carbohydrates in the oral cavity, where starch molecules get partially digested into oligosaccharides, maltose and glucose.^[12] Previous studies have shown the potential of amorphous SiO_2 nanoparticles to negatively impact the structure and function of lysozyme.^[13] Although there are reports about the use of SiO_2 nanoparticles for the immobilization of amylase,^[14] detailed investigation on the differential effect of food grade SiO_2 nano- and micro-sized particles on the structure and function of HSA is lacking. Further, there are knowledge gaps on the differences among pristine and food matrix interacted nanoparticles on their interaction with digestive enzymes.

We investigated effect of different grades of SiO_2 particles—food grade SiO_2 nanoparticles (FG- SiO_2 -NPs), food grade SiO_2 microparticles (FG- SiO_2 -MPs) and non-food grade SiO_2 nanoparticles (NFG- SiO_2 -NPs)—on the structure and enzyme kinetics of HSA. In addition, pristine particles were compared with those surfaces interacted with pure proteins (BSA) and with food matrix (milk) to evaluate its consequence on HSA function. We report the differential effects of different grades of SiO_2 particles on the structure and function of HSA and effect of surface passivation with BSA.

2 | MATERIALS AND METHODS

2.1 | Chemicals and reagents

All the chemicals and reagents used were of analytical grade. HSA(1000 U mg^{-1}) was purchased from Lee BioSolutions (Maryland Heights, USA). Soluble potato starch, 3,5-dinitrosalicylic acid and *N*- α -benzoyl-DL-arginine 4-nitroanilide hydrochloride (BAPNA) were purchased from Sigma Aldrich (St. Louis, Missouri, USA). Food grade silicon dioxide particles (SiO_2) in nano-size (AEROSIL 200F) and E551 as micron size (SIPERNAT 22) were obtained from Evonik Corporation (NJ, USA). Similar primary size of non-food-grade SiO_2 nanoparticle was selected to compare the effect of the different grade of the particles and it was purchased from Sigma-Aldrich (cat. no. 637238, 10–20 nm particle size (BET), 99.5% trace metals basis) (Missouri, USA). The stock solutions of SiO_2 particles were prepared according to the standard laboratory procedures using deionized (DI) water obtained from Milli-Q system (Millipore Sigma, MA, USA).

2.2 | Physical characterization

All the particles in their pristine state were characterized for their agglomeration size, shape, surface charge, and surface chemistry. The shape and size of the silicon dioxide particles (FG- SiO_2 -NP, FG- SiO_2 -MP and NFG- SiO_2 -NP) were observed by Scanning Electron Microscopy (SEM). For SEM analysis, samples (5 μL of 50 ppm NP dispersion in DI water) were dropped on the SEM stub, dried at room temperature for overnight and were examined at 50 KV accelerating voltage without coating using SEM-SU8230 (Hitachi, Japan).^[15] The hydrodynamic size, polydispersity index and surface charges of particles (pristine and those interacted with proteins) were measured by dynamic light scattering (DLS) using NanoBrook Omni instrument (Brookhaven's, New York, USA) at 25°C at a concentration of 50 ppm in PBS. Samples prepared for the DLS were loaded into a pre-rinsed folded capillary cell and for the zeta potential measurement, voltage of 100 V was applied.^[16]

Attenuated total reflectance-Fourier transform infrared (ATR-FTIR) was used for the identifications of the surface chemistry of SiO_2 particles (ALPHA-P, Bruker, Billerica, MA, USA). For this, 5 μL aliquots of SiO_2 particles (stock concentration 10 mg mL^{-1} in DI water) were dropped on the ATR probe and left to dry for 15 minutes. Wavelength range of 400–4000 cm^{-1} , with a resolution of 4 cm^{-1} , and 24 scans were used for obtaining the FTIR spectrum. Qualitative analysis of Si–O–Si groups (cyclic and linear) was

performed by deconvolution of the FTIR spectra region between 1200 and 900 cm^{-1} using the OMNIC 8.2.0.387 software (Thermo Scientific, MA, USA).

2.3 | Interaction of SiO_2 particles with HSA

A stock solution of HSA (1000 U) was prepared in 20 m_M PBS buffer at pH 6.5 and diluted with the same buffer for the working stock (2 U). Depending on the experiment protocol the concentration of the enzyme was either kept constant and/or varied. The reaction mixture was equilibrated for the optimal incubation time at 37°C for 1 hour to ensure the dynamic equilibrium in the protein corona formation.^[17]

2.4 | Effect of SiO_2 particles on HSA activity and enzyme kinetics

HSA activity was assessed by measuring the amount of reducing sugars generated by the action of HSA on starch (substrate) by dinitrosalicylic acid method (DNS). For this purpose, 10% (w/v) soluble potato starch solution was prepared by dissolving 5 g of potato starch in 50 mL of 20 m_M sodium phosphate buffer (pH 6.9 with 0.006 M of sodium chloride). The resulting solution was heated directly on a hot plate under constant stirring, till boiling and the solution was maintained at that temperature for 15 minutes to enhance the solubility of the starch solution. DNS reagent was prepared by dissolving 1 g of 3,5-dinitrosalicylic acid in 50 mL dH_2O . It was then mixed with sodium potassium tartrate tetrahydrate solution prepared in 2N sodium hydroxide, heated on a hot plate at 70°C and made up to 100 mL with dH_2O . The working solution of standard enzyme HSA (2 U mL^{-1}) was prepared from stock solution (1000 U mL^{-1}) in PBS buffer and used to hydrolyze the starch. The HSA inhibitory activity of silica particles and tannic acid (as the positive control) were determined according to the procedure described earlier with modifications.^[18] The inhibitors (SiO_2 particles and tannic acid) (40 μL of 2 mg mL^{-1}) and HSA (40 μL) were added in the 96 well microplate and incubated at 37°C for 1 hour. Subsequently, 20 μL of starch solution was added to the wells, incubated for 10 minutes at 37°C and the reaction was terminated by adding 100 μL of DNS reagent and keeping the plate in boiling water bath maintained at 100°C for 15 minutes. The plate was cooled to room temperature and the absorbance was measured at 540 nm for each well using a plate reader (Spectra max i3x, Molecular Devices, USA). The % of amylase inhibition were calculated using

following equation:

$$\begin{aligned} & \% \text{ of Amylase Inhibition} \\ &= \frac{(\text{negative control activity}) - (\text{sample activity})}{\text{negative control activity}} \\ & \times 100\% \end{aligned}$$

where reaction mixer without the presence of any particles or inhibitor was taken as negative control.

The effect of particles on enzyme kinetics was elucidated by measuring enzyme activity in particles interacted HSA at increasing concentrations of soluble starch. Kinetic parameters were obtained by incubating 2 U mL^{-1} HSA with incremental concentrations of inhibitors (SiO_2 particle from 2 to 16 mg mL^{-1}) and the substrate (starch) concentration (from 1 to 10 mg mL^{-1}). Types of enzyme inhibition when interacted with particles were determined by fitting the kinetic data in to Dixon plot and Cornish-Bowden plot graphs.

2.5 | HSA- SiO_2 particles interaction: Determining enzyme binding constant

The binding constants for HSA interactions with different SiO_2 particles were determined by measuring fluorescence intensity of protein. Samples for fluorescence spectroscopy were prepared by mixing 100 μL of HSA (10 U mL^{-1}) with 30 μL of increasing concentration of the SiO_2 particles from 0.5 to 10 mg mL^{-1} . The resulting mixture was then incubated at 37°C for 1 hour. Fluorescence measurements were obtained using a plate reader (Spectra max i3x, Molecular Devices, USA). The emission spectra were recorded in the range of 320–600 nm upon excitation with 280 nm, using 10 nm/10 nm slit widths, and each spectrum was the average of three scans.

The binding constant and number of binding sites were obtained by Stern-Volmer equation:

$$\frac{I_0}{I} = 1 + K_q \tau_0 [Q] = 1 + K_{sv} [Q]$$

where I_0 and I represent the fluorescence intensities in the absence and the presence of the quencher (SiO_2 Particles), respectively, K_{sv} is the dynamic quenching constant and Q is the concentration of the quencher. The slope of the fitted data to the equation gives the value of K_{sv} . k_q is the bimolecular quenching rate constant, and τ_0 is the biomolecular fluorescence lifetime in the absence of quencher, which is considered to be 2.97 ns for α -amylase.^[19]

2.6 | Circular dichroism spectroscopy

SiO₂ particles were interacted with HSA (final concentrations of 1 mg mL⁻¹ and 0.15 mg mL⁻¹, respectively) in 20 mM phosphate buffer (pH 6.5) for 1 hour at 37°C. Four hundred microliters of the HSA-particle complex solution was added to a quartz cell with 0.1 cm path length, and the CD spectra were recorded from 190 to 260 nm at 37°C using a Jasco J-810 Spectro-polarimeter (Jasco Corp., OK, USA). Each spectrum was an average of three scans, and the percentages of helices, strand, turns, and unordered were calculated using the DICHROWEB online software (DWA03771307) at <http://www.cryst.bbk.ac.uk/cdweb> (access date 16/05/2018).

2.7 | Effect of BSA and milk interacted SiO₂ particles on HSA activity

SiO₂ nanoparticles exposed to the food matrix/pure protein were hypothesized to lower their inhibitory action on HSA. In order to verify this effect, SiO₂ particles were prior exposed to skimmed milk obtained from a local grocery store (Quebon, Agropur Dairy Cooperative, QC, Canada). Milk stored at 4°C was subjected to centrifugation (14,000 rpm for 15 minutes) and the supernatant was collected for further studies. Two hundred microliters of 10 mg mL⁻¹ of particles were mixed with 800 μL processed milk or 800 μL of 1 mg mL⁻¹ BSA (control) and incubated for 1 hour at 37°C. Higher concentration of particles were chosen to maximize the protein corona formation. Particles were then pelleted out by centrifugation (14,000 rpm), excess of milk or BSA in the supernatant was discarded. The washing step was repeated 3 times by suspending particles in phosphate-buffered saline (PBS) and pelleting by centrifugation. The milk/protein interacted particles were used to test HSA enzyme activity using DNS method as described in the preceding section.

2.8 | Protease activity of milk interacted SiO₂ particles

The milk interacted particles were prepared the same way as described above. After the last wash, the pellet was added with 500 μL of substrate—*N*-α-benzoyl-DL-arginine 4-nitroanilide hydrochloride (BAPNA)—prepared in 50 mM Tris HCl buffer, pH 8.0, and containing 20 mM CaCl₂. After addition of BAPNA (0.6 mg mL⁻¹) the pellet containing milk interacted SiO₂ particles were suspended by vortexing. The solution was kept at 37°C for overnight.

Subsequently, the absorbance of the supernatant was measured at 420 nm using a UV-vis spectrophotometer (Spectra Max M2, Molecular Devices, USA) after removing particles from the suspension by centrifugation at 14,000 rpm for 15 minutes. The obtained absorbance value was used in line equation obtained from standard curve for measuring the level of protease activity in milk interacted particles.

2.9 | Statistical analysis

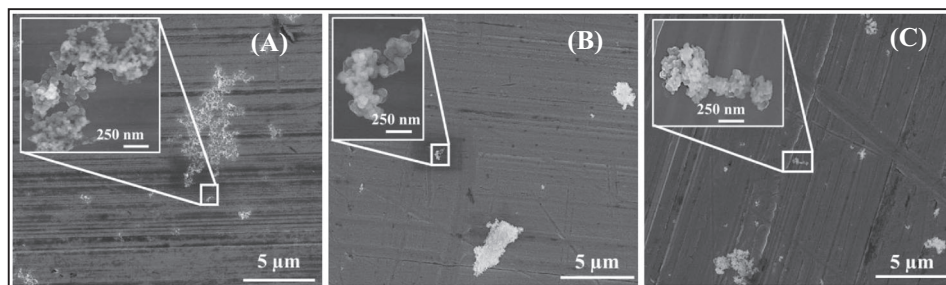
Experiments were performed in triplicates and replicated at least three times. The data collected in this study are expressed as the mean value ± standard deviation (SD). Statistical comparisons were made by Duncan and *P* value ≤0.05 was considered significantly difference.

3 | RESULTS

In this study, FG-SiO₂-NPs, FG-SiO₂-MPs and NFG-SiO₂-NPs were characterized prior to their interaction with the HSA enzyme to assess their size and shape using SEM as shown in the Figure 1A–C. According to the suppliers, the primary particle sizes of FG-SiO₂-NP, FG-SiO₂-MP and NFG-SiO₂-NP were 12 nm, 110 μm and 20 nm, respectively. However, results of FG-SiO₂-NP from SEM analysis showed agglomerates of spherically shaped particles, and the average diameter of primary particle was around 30 nm (Figure 1A). FG-SiO₂-MP (E551) and NFG-SiO₂-NP had primary particles of size ~30 nm which were aggregated to form particle aggregates of size 0.5–5 μm (Figure 1B and C). The difference in hydrodynamic size when suspended in buffer was evident among these particles as 274, 602, and 1046 nm for FG-SiO₂-NP, FG-SiO₂-MP, and NFG-SiO₂-NP, respectively (tabular data, Figure 1D). The increase in hydrodynamic size of protein interacted particles suggested protein corona formation on the particles. All tested particles exhibited negative surface charge.

3.1 | The surface chemistry of different grades of SiO₂ particles

The surface chemistry of different grades of pristine SiO₂ particles were compared using FTIR spectra (Figure 2). These spectra were measured in full scan from 4000 to 400 cm⁻¹, and the region between 1200 and 900 cm⁻¹ was Fourier self-deconvoluted in order to identify the ring, branched and liner structure of siloxane and silanol



(D)	Hydrodynamic size	Polydispersity index	Zetapotential [mV]
	[nm ± Std dev]	[PdI ± Std dev]	± Std dev]
FG-SiO ₂ -NP	274.42 ^a (±4.2)	0.277 ^a (±0.008)	-21.9 ^{b,c} (±6.3)
FG-SiO ₂ -MP	602.16 ^a (±17.8)	0.356 ^a (±0.02)	-25.02 ^{a,b} (±3.3)
NFG-SiO ₂ -NP	1046.16 ^{a,b} (±38.0)	0.494 ^{a,b} (±0.06)	-24.09 ^{a,b} (±0.5)
BSA-FG-SiO ₂ -NP	3218.26 ^c (±119.3)	0.46 ^b (±0.02)	-18.13 ^{b,c} (±4.8)
BSA-FG-SiO ₂ -MP	4460.69 ^d (±1437.5)	0.507 ^b (±0.02)	-30.18 ^{a,b} (±6.2)
BSA-NFG-SiO ₂ -NP	2632.78 ^{b,c} (±231.2)	0.361 ^a (±0.02)	-21.43 ^{b,c} (±0.9)
Milk-FG-SiO ₂ -NP	827.49 ^a (±80.9)	0.293 ^a (±0.03)	-16.21 ^c (±2.4)
Milk-FG-SiO ₂ -MP	269.31 ^a (±15.8)	0.312 ^a (±0.04)	-16.53 ^c (±0.8)
Milk-NFG-SiO ₂ -NP	1066.62 ^{c,b} (±76.9)	0.387 ^{a,b} (±0.02)	-18.38 ^{b,c} (±1.5)

FIGURE 1 SEM images of SiO₂ particles obtained after atmospheric drying of particle suspensions (50 ppm) on SEM stub. Images were obtained using SEM (Hitachi, SEM-SU8230) without coating. (A) FG-SiO₂-NP (B) FG-SiO₂-MP and (C) NFG-SiO₂-NP. (D) hydrodynamic diameter, polydispersity index and surface charge of SiO₂ particles in the presence and absence of proteins suspended in PBS were determined using DLS. Means with different small letters in the same column are significantly different (Duncan, $P < 0.05$)

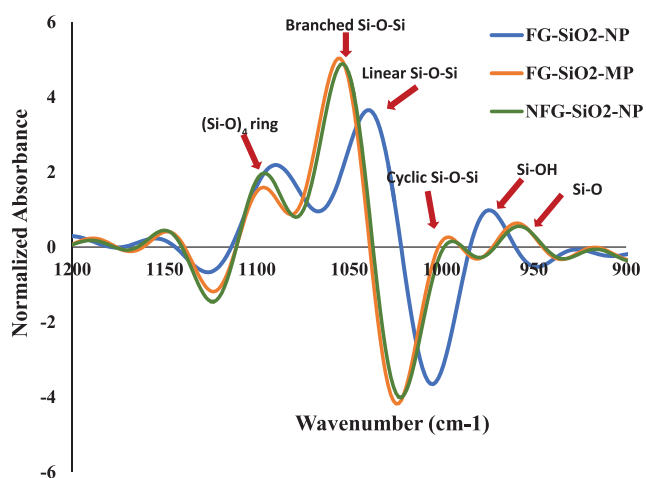


FIGURE 2 FTIR analysis of SiO₂ particles. Particles suspended in water were dropped and dried on the ATR probe before taking the spectra for a wavenumber range of 400–4000 cm⁻¹ using ATR-FTIR. The spectra were generated by Fourier self-deconvolution of wavenumber between 1200 and 900 cm⁻¹

groups. Core of the SiO₂ particles contain siloxane (Si-O-Si) rings and silanol (Si-OH) groups are found on the surface of the particles. As presented in Figure 2, more Si-OH groups (963 cm⁻¹)^[15,20] were detected in FG-SiO₂-NP while higher Si-O groups (940 cm⁻¹) were identified in the FG-SiO₂-MP and NFG-SiO₂-NP. The branched siloxane group (at 1050 cm⁻¹) was present in FG-SiO₂-MPs and NFG-SiO₂-NPs with similar intensity. Most of the siloxane groups in FG-SiO₂-NP existed as linear structure (1030 cm⁻¹)^[15,21] while cyclic structures (1000–1020 cm⁻¹)^[15,22] were noted in FG-SiO₂-MPs and NFG-SiO₂-NPs.

3.2 | Enzyme kinetics studies

The inhibition of HSA activity was determined by DNS method and the inhibition of HSA by silica particles were compared with positive control (tannic acid) (Figure 3A).

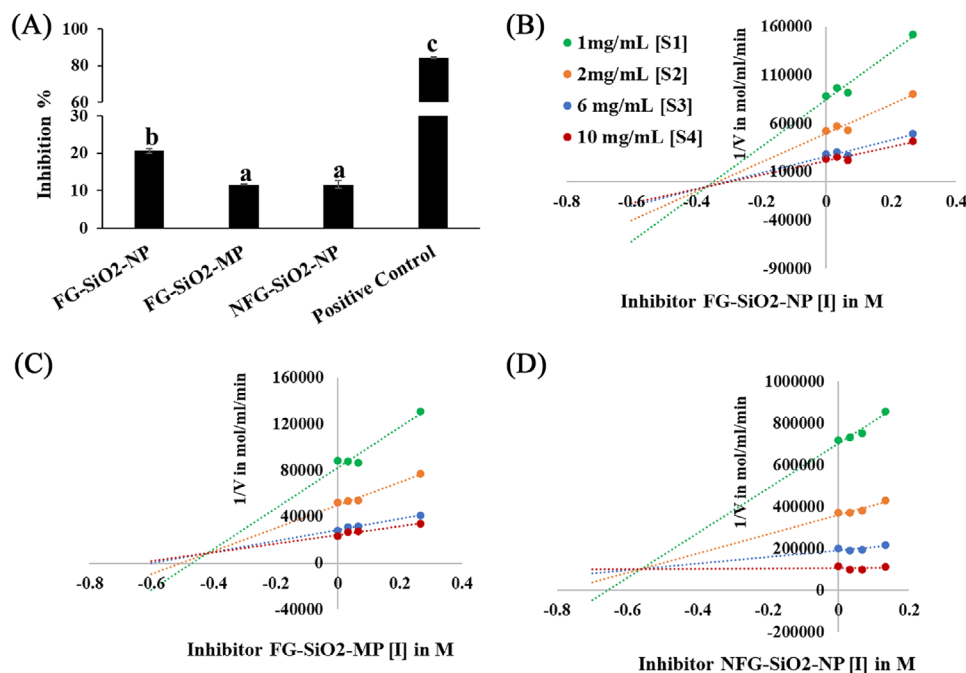


FIGURE 3 (A) HSA inhibition (%) activity of pristine SiO₂ particles. Average values plotted in the graph with different small letters indicate significant difference (Duncan, $P < 0.05$). Dixon plot was developed by following enzyme activity with increasing concentration of silica particles at incremental concentrations of substrate (starch) (B) FG-SiO₂-NP, (C) FG-SiO₂-MP, (D) NFG-SiO₂-NP

It was found that the inhibition was higher when the enzyme interacted with FG-SiO₂-NP followed by NFG-SiO₂-NP and FG-SiO₂-MP (Figure 3A). We observed 20% reduction in HSA activity when it was interacted with FG-SiO₂-NP while the inhibition was only ~10% for the enzyme interacted with FG-SiO₂-MP and NFG-SiO₂-NP at comparable concentrations of particles. The dissociation constant (K_i) for enzyme-inhibitor complex was obtained using Dixon plot. The effect on the enzyme rate of HSA was determined at increasing substrate concentration from 1 to 10 mg mL⁻¹ and over a range of inhibitor (FG-SiO₂-NP, FG-SiO₂-MP and NFG-SiO₂-NP particles) concentration from 2 to 16 mg mL⁻¹. The type of enzyme inhibition was deduced from Dixon plot given in Figure 3B, C, and D wherein the inhibition constant K_i is the concentration required to produce half maximum inhibition that suggest the potency of an inhibitor.

The FG-SiO₂-NP interacted HSA (Figure 3B) showed non-competitive inhibition as the inhibition curves obtained with different substrate concentrations converged below the x axis. The value of [I] where they intersect is typical of non-competitive type inhibition with the K_i value of 0.4 M. The types of inhibition were also confirmed by Cornish-Bowden plot (Supplementary Information 1A) which intercepted below the x axis.^[23] HSA interacted with FG-SiO₂-MP and NFG-SiO₂-NP

showed a mixed type inhibition as the lines converged above the x axis and the value of [I] where they intersect was at K_i value of 0.45 M (Figure 3C and D).^[24]

3.3 | Fluorescence quenching studies of HSA in the presence of SiO₂ particles

Quenching of protein's intrinsic (tryptophan) fluorescence was employed for more detailed understanding of protein-particle interactions. HSA showed strong fluorescence emission at 360 nm when excited with 280 nm. The fluorescence value gradually decreased along with increasing concentrations of SiO₂ particles. As expected, fluorescence quenching was relatively higher for HSA interacted with FG-SiO₂-NP compared to that of FG-SiO₂-MP and NFG-SiO₂-NP (Supplementary Figure, SI3). Stern-Volmer (SV) equation was applied to determine the nature of fluorescence quenching after interaction of HSA with SiO₂ particles. K_{SV} were calculated for FG-SiO₂-NP, FG-SiO₂-MP and NFG-SiO₂-NP interacted HSA from SV plot and values were 1.5454, 0.3177, and 0.359 M⁻¹, respectively (Table 1). Similarly, the biomolecular quenching rate constant K_q for HSA interacted with FG-SiO₂-NP, FG-SiO₂-MP and NFG-SiO₂-NP were 5.2×10^8 , 1.07×10^8 , and 1.21×10^8 (M⁻¹ s⁻¹), respectively (Table 1).

TABLE 1 Table summarizing binding affinity of HSA: Stern-Volmer constants (K_{sv}) and biomolecular quenching rate parameter (K_q) of HSA in the presence of SiO_2 particles calculated from Stern-Volmer plot given in Supplementary Information 3

	K_{sv} [M^{-1}]	K_q [$\text{M}^{-1}\text{s}^{-1}$]
FG- SiO_2 -NP	1.5454	5.2×10^8
FG- SiO_2 -MP	0.3177	1.07×10^8
NFG- SiO_2 -NP	0.359	1.21×10^8

$\tau_0 = 2.97 \times 10^{-9}$ s for trypsin in the absence of quencher.

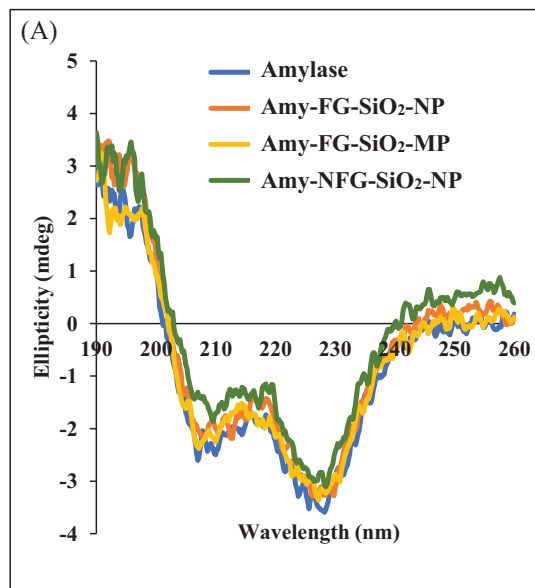
3.4 | Circular dichroism spectroscopy to understand the changes in the secondary structure of HSA during interaction with SiO_2 particles

The Circular dichroism (CD) spectroscopy was used to determine changes in the secondary structure of HSA upon interaction with SiO_2 particles. The typical pattern of α -helical protein with negative band at 222 and 208 nm and a positive band at 190 nm secondary structure pattern^[25] was observed (Figure 4A). Tabular data (Figure 4B) summarizes percentage of prominent secondary structure features of HSA with and without SiO_2 particles interaction. Based on the spectra, the secondary structure of SiO_2 particles interacted HSA was only slightly different from free HSA. Generally, the percentage of helix and unordered structures were reduced by the interactions of HSA with SiO_2 particles while the percentage of strand and turns increased. The alteration in secondary structure as evidenced by the reduction in helix and increase in turns was comparatively higher when HSA was interacted with SiO_2 nanoparticles (Figure 4B).

We hypothesized that the inhibitory effect of pristine SiO_2 particles on HSA could be ameliorated by pre-treatment of particles with albumin and food matrix. Bovine serum albumin was used as the pure protein to coat pristine SiO_2 particles while skimmed milk (0% fat) obtained from a local grocery store was used as a model food matrix.

3.5 | Impact of protein interacted SiO_2 particles on HSA activity

The HSA inhibition activities of pure protein and milk interacted SiO_2 were evaluated, and the results are shown in Figure 5. Characteristic FTIR peak at 1500–1700 cm^{-1} confirmed the presence of proteins on the surface of BSA and milk interacted particles (Supplementary Information 2). The inhibitory action of SiO_2 particles on HSA decreased significantly when the particles were precoated with BSA before interacting with HSA (Figure 5A).



(B)	Helix (%)	Strand (%)	Turns (%)	Unordered (%)
Amylase	4.8	35.6	18.3	41.3
Amy-FG- SiO_2 -NP	4.6	36.6	18.8	40.1
Amy-FG- SiO_2 -MP	4.6	35.7	18.6	41.3
Amy-NFG- SiO_2 -NP	4.2	37.2	19.0	39.7

FIGURE 4 (A) CD spectra of HSA in the presence and absence of SiO_2 particles. (B) Table summarizes the secondary structure features of HSA assessed using CD after interacting with SiO_2 particles. The concentration of HSA and the SiO_2 Particles in the CD study was 0.15 and 1 mg mL^{-1} , respectively

Among the tested particles, FG- SiO_2 -NP showed the most significant difference when interacted with BSA. While, the pristine FG- SiO_2 -NP showed 12% inhibition of HSA activity, it was only 6% when protein interacted FG- SiO_2 -NP was used (50% recovery). Contradictory to our expectations, however, milk interacted SiO_2 particles had higher HSA inhibition in comparison to pristine SiO_2 particles (Figure 5A). The increase in HSA inhibition was evident in FG- SiO_2 -MP, where ~ 2.5 -fold increase in HSA inhibition was observed for milk interacted particles in comparison to the inhibition of HSA by pristine particles.

We suspected that the increase in HSA inhibition shown by milk interacted particles is because of the presence of protease enzyme in the biocorona. Therefore, we measured the protease enzyme activity of milk interacted SiO_2 particles. As shown in Figure 5B, the protease activities on milk interacted SiO_2 particles (2 mg) were shown to be ~ 30 mU for FG- SiO_2 -NP and FG- SiO_2 -MP. Among the particles, food-grade particles had the highest level of protease

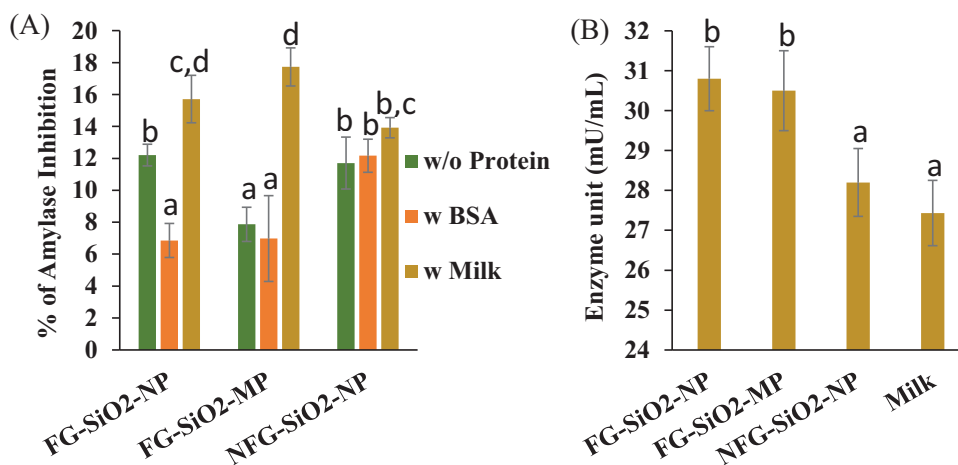


FIGURE 5 Impact of protein interacted SiO₂ particles on HSA activity. (A) HSA enzyme inhibition activity of pristine SiO₂ particles, BSA interacted SiO₂ particles, and milk interacted SiO₂ particles (B) activity of protease on milk interacted SiO₂ particles. Means with different small letters are significantly different (Duncan, $P < 0.05$)

activity. Notably, the protease activity on particles interacted milk was higher than that from the same concentration of milk—the enhancement of protease activity—suggestive of protease enrichment on the surface of particles.

4 | DISCUSSION

HSA constitutes a significant proportion of salivary proteins and plays an important role in the initial digestion of starch, glycogen, and other polysaccharides in mouth. Previous studies from our group had reported the preferential binding of amylase onto dietary nanoparticles.^[26] As a sequel to that study, we were interested in assessing the consequences of amylase binding onto particle surface on its structure and function. In addition, we were interested in understanding if the effect could be different when nanoparticles surfaces are modified by food metrics. This study revealed the differential effects of food grade SiO₂ nanoparticles, microparticles, and non-food grade SiO₂ nanoparticles on HSA activity and that surface modification by food matrix could influence its effect on amylase activity.

Among the tested particles, nanoparticles of food grade SiO₂ showed the highest level of HSA inhibition (Figure 3A). HSA inhibition was concentration dependent, and we followed the inhibition kinetics of particle interacted. Our analysis showed difference among particles in the type of HSA inhibition where FG-SiO₂-NPs showed a non-competitive type inhibition while micro-sized and the non-food grade SiO₂ nanoparticles showed a mixed type inhibition (Figure 3B, C, and D). Non-competitive

inhibition is a type of mixed inhibition involving enzyme-substrate-inhibitor complex while in a competitive binding, the inhibitor (particle in this case) precludes the binding of substrate. We also noticed that the protein binding affinity of food grade SiO₂ nanoparticles to be relatively higher in comparison to other particles (Table 1 and Supplementary Information 3). The K_q (binding affinity) value for food grade SiO₂ nanoparticles was ~5 times higher than that of micron particles and non-food grade SiO₂ nanoparticles. The outcomes from enzyme inhibition assay was found to be in line with the binding affinity data where stronger affinity of FG-SiO₂-NPs corresponded with higher inhibition of the HSA. Moreover, the quenching effect of FG-SiO₂-NP was found to be concentration dependent whereas, there was no significant fluorescence quenching with increasing concentration of FG-SiO₂-MP and NFG-SiO₂-NP (Supplementary Information 3). The fluorescence quenching is also an indicator of the change in the tertiary structure of proteins.^[27] Interestingly, as observed by CD spectroscopy there was no drastic change in the secondary structure of HSA when interacted with different grades of SiO₂ particles (Figure 4). Taken together, these results suggest that the interaction of particles with HSA has minimal effect on secondary structure but changes their tertiary structure where the effect was higher for FG-SiO₂-NPs. Thus, while we observed a negative impact of food grade SiO₂ particles on the function and binding affinity for HSA, there are studies reporting the potential of using SiO₂ nanoparticles for the immobilization of enzymes. For instance, SiO₂ particles are reported to immobilize amylase for applications in laundry detergents^[14] and modified magnetic nanoparticles to increase the thermal stability and enzyme activity

of amylase.^[28] These reported studies and our observation that different grades of SiO₂ nanoparticles (food grade and non-food grade) showed different levels of HSA inhibition despite their comparable size are suggestive of factors other than particle size involved in determining binding affinity and inhibition of HSA. We argue that the differences in enzyme inhibition and binding affinities could be explained based on the differences in the surface chemistry of these materials and how it responds to features of HSA.

According to Zhuravlev model, the presence of silanol groups and siloxane bridges are the factors determining surface properties of amorphous SiO₂.^[29] The negative surface charge (of pristine SiO₂ particles) and hydrophilic nature of silanol groups (at neutral pH) and hydrophobic nature of siloxane ring structure provide anchoring points for proteins on SiO₂ particles. As observed by FTIR spectra, FG-SiO₂-NPs have higher Si–OH groups on their surfaces in comparison to NFG-SiO₂-NPs and FG-SiO₂-MPs (Figure 2). In addition, the higher content of branched and cyclic siloxane groups on the surface of FG-SiO₂-MPs and NFG-SiO₂-NPs differentiated them from FG-SiO₂-NPs in terms of surface chemistry. The outcome of protein-particle interactions, however, are dictated by how the surface chemistry of SiO₂ particle interact with unique features of proteins defined by charge, hydrophobicity, and divalent cation binding sites etc. HSA structure consists of three domains (A, B and C); of which the catalytic amino acid residues (Asp197, Glu233 and Asp 300) is located in domain A.^[30] In addition, domain A has a chloride ion coordinated by side chains of Arg 195, Asn 298, and Arg 337 and a calcium ion that is coordinated by His201 from domain A and Asn100, Arg158, and Asp167 from domain B.^[30] The calcium ion by virtue of its location stabilizes the structural integrity of the A and B domains, orients the His 101 in the substrate-binding cleft and provides an asymmetric environment for substrate binding.^[31] The chloride ion is assumed to play a role in stabilizing the structural organization of catalytic residues by diminishing the possibility of non-productive and unfavorable electrostatic interactions that otherwise might exist between basic and acidic residues located in the active-site region.^[30] Given the relevance of calcium and chlorine binding motifs in binding on to nanoparticles, it is likely that binding of HSA molecules to SiO₂ particles disrupt the structural integrity of A and B domains and the substrate binding. The relative amounts of silanol groups and siloxane groups on different particles differentiate the extent and type of enzyme inhibition. Thus, while more studies are warranted on the molecular interactions of amylase with SiO₂ nanoparticles, we reason that FG-SiO₂-NP with relatively higher silanol groups disrupt molecular structure of HSA and affirm the binding through hydrophilic interactions leading to non-competitive type of amylase inhibition.

From our studies it was obvious that HSA inhibition require direct interaction of SiO₂ surface with protein molecule. Therefore, we argued that pristine SiO₂ particles modified by surface adsorbed proteins and other biomolecules, as in the case of those incorporated in food, would ameliorate HSA inhibition by silica particles. We tested this hypothesis by surface modification of pristine SiO₂ particles with either pure proteins (BSA) or those suspended and recovered from skimmed milk (as a model food matrix). As expected, the surface modification of SiO₂ particles using BSA decreased the HSA inhibitory potential of particles (Figure 5A). The formation of BSA layer (as confirmed with DLS and FTIR) over the surface of SiO₂ particles precludes the direct interaction of HSA with SiO₂ surface chemistry. The potential of albumin as a binding partner of HSA was reported recently.^[32] Thus, the protein-protein interaction that does not compromise the function is thought to anchor HSA onto these particles but without major disruption in its function.

Silica particles applied in food are likely to acquire surface coating of biomolecules before its likely interaction with HSA. As such, it is unlikely that the pristine surface of silica particles would interact with HSA. While this could be in most of the cases of SiO₂ used in food, we tested SiO₂ particles retrieved from milk (pasteurized skimmed milk) for their effect on HSA. Contradictory to the effect of BSA, particles interacted with milk showed a higher HSA inhibition (Figure 5A). Based on results from the BSA interacted particles, we ruled out the possibility of the disruption of the structure of HSA. We suspected the presence of protease in the biocorona of SiO₂ particles retrieved from milk. The protease presents these particles could digest HSA which will be observed as decreased HSA activity. Our investigations in fact showed the presence of protease activity in milk interacted particles (Figure 5B). This observation exemplifies possibilities of undesired outcome arising from unexpected phenomena when nanoparticles interact with food matrix.

5 | CONCLUSION

In conclusion, our studies delineated differential effect of different grades of SiO₂ particles to bind with HSA and their effect on the structure and function of HSA. Among different grades of SiO₂ tested, FG-SiO₂-NP showed higher binding affinity, potential disruption of tertiary structure and partial loss of enzyme function. Our studies showed that direct interaction of SiO₂ nanoparticles with HSA is needed for the alteration in structure and function of HSA and that effect could be shielded by modifying the surface of SiO₂ particles. These studies also showed that the food matrix interacted particles can affect the

functionality of HSA differently depending on the type of food matrix. Outcome from this study signifies the molecular interaction between digestive enzymes and dietary nanoparticles that could cause potential adverse effects on nutrient assimilation.

ACKNOWLEDGMENT

We acknowledge funding from NSERC RGPIN-2017-04727 and CRC/George/X-coded/248475 for supporting this research work.

CONFLICTS OF INTERESTS

The authors declare no conflicts of interest.

ORCID

Wut Hmone Phue  <https://orcid.org/0000-0003-2414-0086>

REFERENCES

- L. J. Frewer, N. Gupta, S. George, A. R. H. Fischer, E. L. Giles, D. Coles, *Trends Food Sci. Technol.* **2014**, *40*, 211.
- C. McCracken, P. K. Dutta, W. J. Waldman, *Environ. Sci.: Nano*, **2016**, *3*, 256.
- M. I. Setyawati, C. Y. Tay, D. T. Leong, *Small*, **2015**, *11*, 3458.
- J. J. Powell, N. Faria, E. Thomas-McKay, L. C. Pele. *J. Autoimmun.* **2010**, *34*, J226.
- S. Bettini, E. Boutet-Robinet, C. Cartier, C. Coméra, E. Gaultier, J. Dupuy, N. Naud, S. Taché, P. Grysan, S. Reguer, N. Thieriet, M. Réfrégiers, D. Thiaudière, J.-P. Cravedi, M. Carrière, J.-N. Audinot, F. H. Pierre, L. Guzylack-Piriou, E. Houdeau. *Sci. Rep.*, **2017**, *7*, 40373.
- M. Winter, H.-D. Beer, V. Hornung, U. Krämer, R. P. F. Schins, I. Förster. *Nanotoxicology*, **2011**, *5*, 326.
- N. G. Lamson, A. Berger, K. C. Fein, K. A. Whitehead, *Nat. Biotechnol.* **2019**, *4*, 84.
- M. Younes, P. Aggett, F. Aguilar, R. Crebelli, B. Dusemund, M. Filipič, M. J. Frutos, P. Galtier, D. Gott, U. Gundert-Remy, G. G. Kuhnle, J.-C. Leblanc, L. I. Therese, P. Moldeus, A. Mortensen, A. Oskarsson, I. Stankovic, I. Waalkens-Berendsen, R. A. Woutersen, M. Wright, P. Boon, D. Chrysafidis, R. Gürtler, P. Mosesso, D. Parent-Massin, P. Tobback, N. Kovalkovicova, A. M. Rincon, A. Tard, C. Lambré, EFSA Panel on Food Additives and Nutrient Sources added to Food (ANS), et al. *EFSA J.*, **2018**, *16*, e05088.
- D. Docter, D. Westmeier, M. Markiewicz, S. Stolte, S. K. Knauer, R. H. Stauber, *Chem. Soc. Rev.*, **2015**, *44*, 6094.
- P. C. Ke, S. Lin, W. J. Parak, T. P. Davis, F. Caruso, *ACS Nano*, **2017**, *11*, 11773.
- S. Jafari, H. Derakhshankhah, L. Alaei, A. Fattahi, B. S. Varnamkhasti, A. A. Saboury, *Biomed. Pharmacother.*, **2019**, *109*, 1100.
- P. J. Butterworth, F. J. Warren, P. R. Ellis, *Starch-Stärke*, **2011**, *63*, 395.
- A. A. Vertegel, R. W. Siegel, J. S. Dordick, *Langmuir*, **2004**, *20*, 6800.
- M. Soleimani, A. Khani, K. Najafzadeh, *J. Mol. Catal. B: Enzym.*, **2012**, *74*(1), 1–5.
- W. H. Phue, M. Liu, K. Xu, D. Srinivasan, A. Ismail, S. George, *J. Agric. Food Chem.* **2019**, *67*, 12264.
- S. George, H. Gardner, E. K. Seng, H. Chang, C. Wang, C. H. Yu Fang, M. Richards, S. Valiyaveetil, W. K. Chan, *Environ. Sci. Technol.* **2014**, *48*, 6374.
- S. Tenzer, D. Docter, J. Kuharev, A. Musyanovych, V. Fetz, R. Hecht, F. Schlenk, D. Fischer, K. Kiouptsi, C. Reinhardt, K. Landfester, H. Schild, M. Maskos, S. K. Knauer, R. H. Stauber, *Nat. Nanotechnol.*, **2013**, *8*, 772.
- W. Lou, Y. Chen, H. Ma, G. Liang, B. Liu, *J. Food Sci. Technol.* **2018**, *55*, 3640.
- M. A. Castanho, M. J. Prieto, *Biochim. Biophys. Acta*, **1998**, *1373*, 1.
- R. E. Saputra, Y. Astuti, A. Darmawan, *Spectrochim. Acta, Part A*, **2018**, *199*, 12.
- A. Darmawan, L. Karlina, Y. Astutia, Sriatun, J. Motuzas, D. K. Wang, J. C. Dinizda Costa, *J. Non-Cryst. Solids*, **2016**, *447*, 9.
- J. - Y. Bae, J. Jang, B. - S. Bae, *J. Sol-Gel Sci. Technol.*, **2017**, *82*, 253.
- A. Cornish-Bowden, *Biochem. J.*, **1974**, *137*, 143.
- V. Krupyanko, *Eur. Chem. Bull.*, **2015**, *4*, 142.
- G. Holzwarth, P. Doty, *J. Am. Chem. Soc.*, **1965**, *87*, 218.
- D. Srinivasan, W. H. Phue, K. Xu, S. George, *NanoImpact*, **2020**, 100238.
- Y. Chen, M. D. Barkley, *Biochemistry*, **1998**, *37*, 9976.
- N. Rasouli, N. Sohrabi, E. Zamani, *Phys. Chem. Res.*, **2016**, *4*, 271.
- L. T. Zhuravlev, *Colloids Surf. A*, **2000**, *173*(1), 1.
- E. A. MacGregor, Š. Janeček, B. Svensson, *Biochim. Biophys. Acta.*, **2001**, *1546*(1), 1.
- N. Ramasubbu, V. Paloth, Y. Luo, G. D. Brayer, M. J. Levine. *Acta Crystallogr D Biol Crystallogr*, **1996**, *52*, 435.
- K. T. B. Crosara, D. Zuanazzi, E. B. Moffa, Y. Xiao, M. A. De A. M. Machado, W. L. Siqueira, *Biomed Res. Int.*, **2018**, *2018*, 6346954.

SUPPORTING INFORMATION

Additional supporting information may be found online in the Supporting Information section at the end of the article.

How to cite this article: Phue WH, Srinivasan D, Hameed A, Yaylayan V, George S. Food grade silica nanoparticles cause non-competitive type inhibition of human salivary α -amylase because of surface interaction. *Nano Select.* 2021;2:632–641. <https://doi.org/10.1002/nano.202000173>